

TEMPERATURE EFFECTS FOR ARRAYED FLEXIBLE pH SENSOR BASED ON IGZO/Al THIN FILMS

Jung-Chuan Chou^{1*}, Min-Siang Huang², You-Xiang Wu³, Siao-Jie Yan³, Cian-Yi Wu³, Si-Hong Lin³, Yi-Hung Liao⁴, and Chih-Hsien Lai⁵

ABSTRACT

In this study, indium gallium zinc oxide (IGZO) was selected as a sensing material for a thin film fabricated on a PET substrate by radio frequency (R.F.) sputtering. The following temperature effects, hysteresis effects and drift effects of the IGZO pH sensor were investigated. The temperatures were set at 15 °C, 25 °C, 35 °C, 45 °C and 55 °C, respectively. The arrayed flexible IGZO pH sensor was able to operate within a wide temperature range and the best average sensitivity was recorded as 59.893 mV/pH with the temperature set at 55 °C. Furthermore, the drift rate and hysteresis voltage at different temperatures were less than 9.857 mV/hr and 25.316 mV, respectively; the arrayed flexible IGZO pH sensor was found to have good stability. In the future, it could replace the use of litmus paper to detect pH values in various fields such as in the field of chemistry and in the food industry.

Keywords: Indium gallium zinc oxide, pH sensor, temperature effect, hysteresis effect, drift effect, sensitivity, stability.

1. INTRODUCTION

Accurate pH values are important parameters in many fields, such as in the fields of chemistry, food production, agriculture and medicine (Zubieta *et al.* 2016). Litmus paper and glass electrodes are commonly used to detect pH values. However, even though litmus paper is simple and inexpensive, the pH values obtained are not always accurate (Khodadoust *et al.* 2015). A traditional glass electrode based on a thin film of metal oxide results in high sensitivity, good stability, a fast response, and a small hysteresis effect, but the disadvantages of using a glass electrode include its high price, large size and fragility. Glass electrodes requires regular and frequent re-calibration before the measurement process (Manjakkal *et al.* 2016; Amiri *et al.* 2016; Uria *et al.* 2016). However, the advantages of a plastic substrate like flexibility and mechanical stability result in sensors not restricted by any shape (Yaqoob *et al.* 2015). In recent years, the mass production of miniaturized flexible sensors has been achieved because of its low cost and mechanical robustness. Rahimi *et al.* (2016) proposed a pH sensor fabricated on a flexible substrate that also had good average sensitivity and linearity. Based on the above, a flexible Polyethylene Terephthalate (PET) substrate was used to fabricate the flexible pH sensor.

In 1970, P. Bergveld proposed an ion-sensitive field-effect transistor (ISFET) using a SiO₂ thin film which showed that the interface potential of the sensing membrane changed when it reacted with an electrolyte solution. Due to variations in the interface potential, different pH values could be distinguished. The pH-ISFET is also an attractive alternative to the glass electrodes due to its low cost and high accuracy (Dong *et al.* 2013; Chen *et al.* 2015). Metal oxide thin films have been applied in various sensor fields, such as in gas sensors (Tyagi *et al.* 2016), pH sensors (Manjakkal *et al.* 2015), glucose biosensors (Nor *et al.* 2015), ultraviolet (UV) sensors (Singh 2016) and so on. Using semiconducting metal oxide films in the sensor fields provides the advantages of simple design, low costs, high sensitivity, and good reproducibility. Amorphous indium gallium zinc oxide (a-IGZO) has been extensively applied in thin-film transistors (TFTs) as the active channel due to its high carrier mobility, high uniformity and long-term stability (Yang *et al.* 2012). IGZO also possesses flexibility due to its amorphous phase (Cho *et al.* 2011) and is a promising material for sensor applications. C.M. Yang *et al.* (2013) proposed the extended-gate field-effect transistor (EGFET) with a nano-IGZO/Al layer and this was applied to the pH sensor.

This article presents research regarding the potentiometric pH sensor based on IGZO/Al sensing membranes. The PET substrate was used to fabricate the arrayed flexible IGZO pH sensor, and the test of its flexibility was investigated in our previous research (Chou *et al.* 2017). The experimental results proved that the PET substrate provided flexibility for the sensor and that the sensor could be used normally even when bent. The IGZO/Al pH sensor was fabricated by radio frequency (R.F.) sputtering and thermal evaporation, and screen-printing technology was used to package the pH sensor. The fabrication process was a simple operation that could allow for mass fabrication at a low cost. The flexible IGZO pH sensor was a semiconductor device easily affected by temperature variation, and the thermal variation also had an effect on the pH stability of the sensing device. In this

Manuscript received May 4, 2019; revised July 2, 2019; accepted July 7, 2019.

^{1*} Professor (corresponding author), Department of Electronic Engineering, National Yunlin University of Science and Technology, Douliu, Taiwan 64002, R.O.C. (e-mail: choujc@yuntech.edu.tw).

² B.S. degree, Department of Electronic Eng., National Yunlin University of Science and Technology, Taiwan 64002, R.O.C.

³ Master student (M.S. degree), Graduate School of Electronic Eng., National Yunlin University of Science and Technology, Taiwan, R.O.C.

⁴ Associate Professor, Dept. of Information and Electronic Commerce Management, TransWorld University, Yunlin, Taiwan 64063, R.O.C.

⁵ Professor, Department of Electronic Eng., National Yunlin University of Science and Technology, Douliou, Tai-wan 64002, R.O.C.

research, average sensitivity and thermal stability were also investigated. Structural analysis was conducted using a field emission scanning electron microscope (FE-SEM) and an atomic force microscope (AFM).

2. EXPERIMENTAL

2.1 Materials

PET was purchased from Uni-Onward Corp. (Taiwan) and used as the substrate of the arrayed flexible IGZO pH sensor. The aluminum ingot was purchased from Summit-Tech Resource Corp. (Taiwan). The IGZO target (99.99% purity and In_2O_3 , Ga_2O_3 , $\text{ZnO} = 1:1:1$) was purchased from Ultimate Materials Technology Co., Ltd. (Taiwan). The silver paste was purchased from Advanced Electronic Materials Inc. (Taiwan). Epoxy was purchased from Sil-More Industrial, Ltd. (Taiwan). All chemicals used in this study were of analytical grade and used without further purification.

2.2 Apparatus

The arrayed flexible IGZO pH sensor was fabricated using two kinds of vacuum equipment, the R.F. sputtering system and the thermal evaporation system. Both sets of vacuum equipment were purchased from I Shien Corporation Co., Ltd (Taiwan). The ultrasonic steri-cleaner used to clean the substrate was purchased from Tun-Hwa Electronic Material Co., Ltd (Taiwan). The oven used for solidifying the silver paste and epoxy resin was purchased from WahFu Precision Co., Ltd (Taiwan). The FE-SEM (Hitachi S4800-I, Japan) came from the Instruments Center at the National Chung Cheng University and was used to measure the thickness of the thin film. The AFM, used to measure the roughness of the IGZO thin film, came from the Instrumentation Center at National Tsing Hua University (Taiwan). The multipurpose X-ray diffractometer (Rigaku D/MAX2500, Japan), used to analyze the crystal structures of sensing membranes, came from the Instrument Center at National Cheng Kung University (Taiwan).

2.3 Fabrication of the arrayed flexible IGZO pH sensor

First, the PET substrate was cleaned using ethanol and then deionized (D. I.) water in an ultrasonic oscillator for 10 min each. Nitrogen was used to remove any residual water from the PET substrate. Next, the aluminum films were deposited on the PET substrate using the evaporation system. The power level and deposition time of the evaporation system were set at 180 W and 90 s, respectively. Then, the IGZO sensing membranes were deposited by R.F. sputtering. The sputtering power, Ar/O_2 flow rate, and the deposition time were 40 W, 16/2 (in sccm), and 30 min, respectively. After that, the conducting wires were fabricated on the PET substrate with silver paste using screen-printing technology and baked at 120 °C in the oven for 30 min. Finally, the epoxy resin was printed on the PET substrate to construct an insulation layer, and define the sensing area (Chou *et al.* 2016). The arrayed flexible IGZO pH sensor is shown in Fig. 1.

2.4 Voltage-time Measurement System

In this study, a voltage-time (V-t) measurement system was used to measure the sensing characteristics of the IGZO pH sensor. The arrayed flexible IGZO pH sensor was connected to the

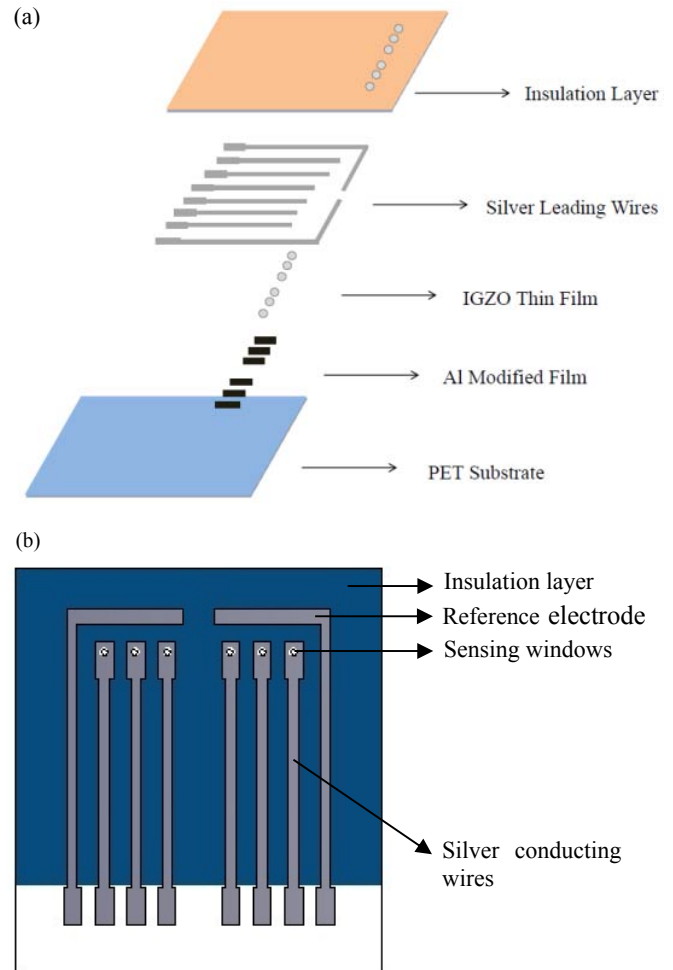


Fig. 1 (a) The fabrication process of the arrayed flexible IGZO pH sensor. (b) The top view of the arrayed flexible IGZO pH sensor.

instrumentation amplifiers (LT1167), and then a data acquisition card (DAQ card) (Model: NI USB-6201, National Instrument Corp., U.S.A.) was used to convert the signal from analog to digital. The read-out circuit was assembled using six of the LT1167, and the response potentials were obtained by measuring the potential difference between the working electrode and the contrast electrode (Chou *et al.* 2013). Finally, the potential signals were processed through a DAQ card, and then the data were transferred to the computer. Analysis software (Model: Lab-VIEW 2011, National Instrument Corp., U.S.A.) was used to obtain the response potentials and the average sensitivity was calculated by Origin 7.0. A prototype of the voltage-time measurement system is shown in Fig. 2 (a) and (b). From the voltage-time measurement system, it is clear that each pair of sensors included two sensing windows and a reference electrode, namely Ag/PET, IGZO/PET, and Ag/PET, respectively. The output voltage of the voltage-time measurement system is expressed in equation 1, and the schematic is shown in Fig. 2 (c).

Fig. 2 (c) shows that the sensing windows, expressed as V_{sen1} , were the accumulation regions for the H^+ ions, and that V_{sen2} was connected to V_{ref} which was connected to the ground level. Formula (1) shows that the reference electrode did not affect the output voltage of the sensing device, and so the reference electrode could be a reference voltage between the working electrode and the contrast electrode.

$$V_{out} = V_{in1} - V_{in2} = (V_{sen1} - V_{ref}) - (V_{sen} - V_{ref}) = V_{sen1} - V_{sen2} \quad (1)$$

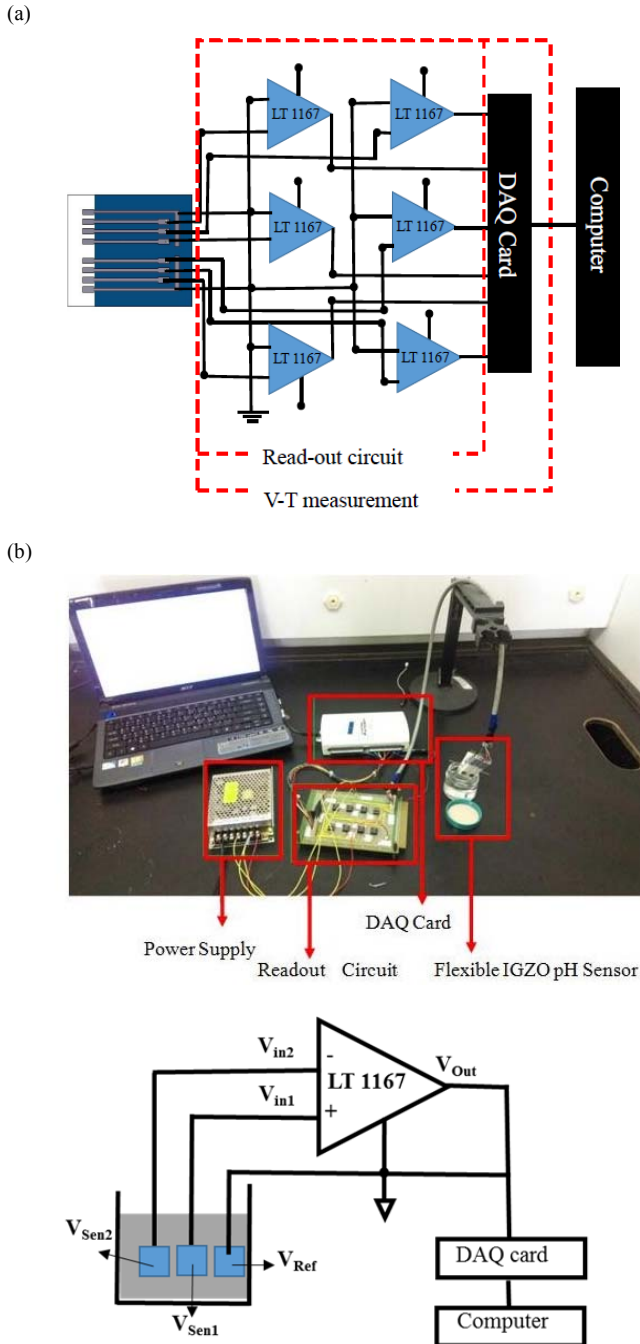


Fig. 2 (a) The prototype of the voltage-time measurement system. (b) the schematic diagram of the flexible IGZO pH sensor. (c) the schematic diagram of input and output of LT1167.

3. RESULTS AND DISCUSSION

3.1 Analysis of the IGZO thin film

This sample was fabricated using thermal evaporation and R.F. sputtering. The thickness of the IGZO film was determined by the Ar/O₂ ratio of the sputtering system, and the Ar/O₂ ratio

was related to the electrical properties of the IGZO thin film (Chen *et al.* 2014; Chou *et al.* 2018). In previous research (Chen *et al.* 2015), the IGZO pH sensor had the best sensing performance when the Ar/O₂ flow ratio was 16/2 (in sccm), and so these deposition parameters were adopted to fabricate the arrayed flexible IGZO pH sensor. The analysis of SEM was used to estimate the thickness of the thin film, and Fig. 3 (a) and (b) present images of the top view and cross-sectional view of the IGZO/Al thin film. As shown in Fig. 3 (a), the IGZO/Al thin film fabricated by thermal evaporation and R. F. sputtering offered high density and excellent uniformity. According to Fig. 3 (b), the thickness of the IGZO thin film and Al thin film were 117 nm and 46 nm, respectively. The material composition was identified through analysis using energy dispersive X-ray spectroscopy (EDX). The results obtained from the EDX mapping in Fig. 4 (a) show that the material was synthesized with the elements In, Ga, Zn, and O. The atomic ratio of the IGZO thin film, analyzed by EDX, was found to be In: Ga: Zn: O = 11.67: 17.02: 9.11: 62.20 atomic percentage (at%). Figure 5 is the AFM image of the IGZO/Al thin film and many peaks can be observed on the surface of the thin film. The average surface roughness of the IGZO/Al thin film was 8.43 nm.

The PET substrate could possibly cause another diffraction due to its flexibility and so the IGZO/Al thin film was deposited on ITO glass for the XRD analysis. The results obtained from XRD are shown in Fig. 6, and make it clear that no IGZO peaks could be observed from the experimental results. Therefore, the evidence confirms that the IGZO thin film had no crystalline phases. In other words, it could be determined that the IGZO thin film was amorphous.

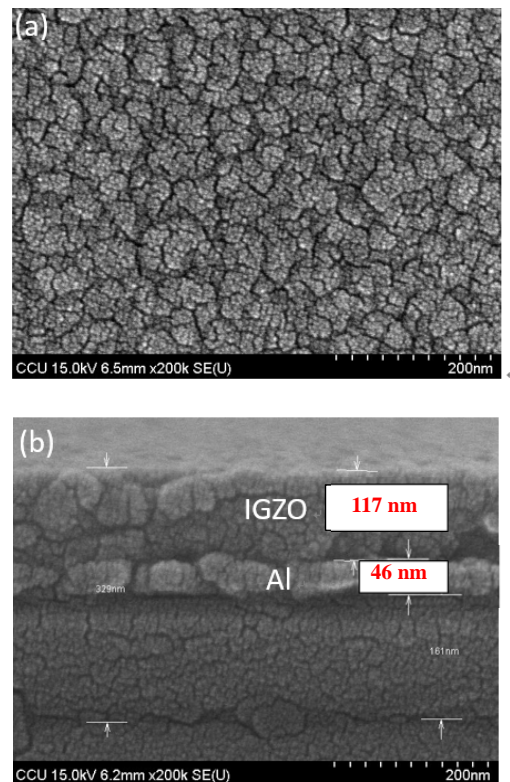


Fig. 3 The image of the FE-SEM for the IGZO/Al thin film (a) top view (b) cross sectional view.

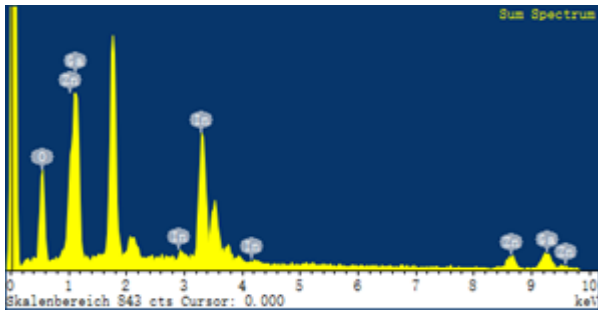


Fig. 4 The EDX spectrum of the IGZO thin film.

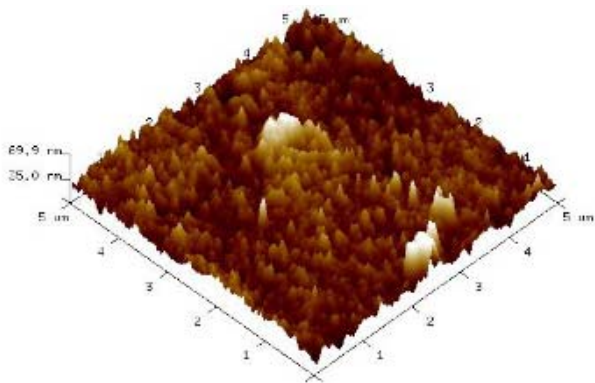


Fig. 5 The image of the AFM for the IGZO/Al thin film.

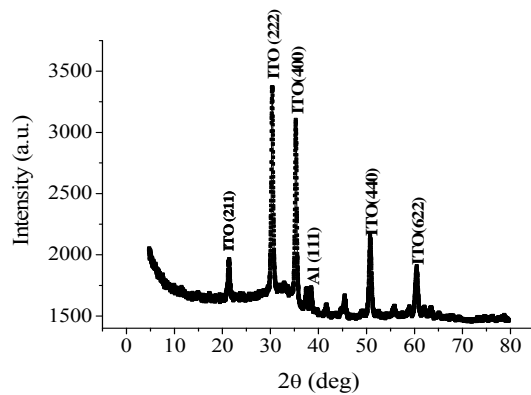


Fig. 6 The XRD analysis spectrum of the IGZO/Al thin film on the ITO glass.

3.2 Influence of the temperature on the sensor performance

In previous research conducted (Chou *et al.* 2016), the sensing properties of the IGZO pH sensor, both with and without the Al membranes, were investigated. Improved sensitivity was attributed to the Al electrode which was used as the signal transmission between the sensing membrane and the measurement system. In this study, the arrayed flexible pH sensor was a potentiometric sensor, so different response potentials were obtained in different pH buffer solutions. The function of the response potential in different pH values can be expressed using the Nernst equation (Sardarinejad *et al.* 2015):

$$E = E^0 - 2.303 \frac{RT}{F} pH \quad (2)$$

where E is the total potential (in V) developed between the sensing and reference electrode. E^0 is the potential of the reference electrode (in V), R is the gas constant ($8.314 \text{ JK}^{-1} \text{ mol}^{-1}$), T is the absolute temperature (in K), and F is Faraday's constant ($9.648 \times 10^4 \text{ Cmol}^{-1}$). From Eq. (2), it is clear that the response potentials were obtained by the temperature and pH values. The term $(2.303 RT)/F$ is called the Nernst slope and in this study; it was also used to express the sensitivity of the pH sensor.

The average sensitivity of the arrayed flexible pH sensor was validated by immersing the pH sensor in different pH buffer solutions from pH 1 to pH 13. Based on formula (2), it was determined that sensitivity had a functional relationship with temperature. In order to investigate the relationship between the average sensitivity and temperature, the pH buffer solution was heated using a thermostatic water bath, and temperatures were controlled at 15 °C, 25 °C, 35 °C, 45 °C and 55 °C, respectively. In the experiment regarding sensing characteristics, five arrayed flexible IGZO pH sensors (Number of sensors, $N = 5$), each containing six sensing windows, were measured under the same conditions. The error bars meaning standard deviation (SD) were obtained from the response potential of six windows of a sensor. The average sensitivity and linearity at different temperatures are listed in Table 1. The average sensitivity values at 15 °C, 25 °C, 35 °C, 45 °C and 55 °C were 48.589 mV/pH, 52.238 mV/pH, 55.446 mV/pH, 56.821 mV/pH, and 58.196 mV/pH, respectively, and the curve of response potential versus pH value at 55 °C is shown in Fig. 7. Table I shows that the experimental results were in good agreement with Eq. (2) because the average sensitivity was proportional to the temperature of the solution. This could be attributed to the fact that an increase in the temperature of a solution increases the mobility of ions in the solution (Sardarinejad *et al.* 2015). An increase in the temperature of a buffer solution would increase the activity of the H^+ ions, and so the surface potential would increase (Sardarinejad *et al.* 2015; Chiang *et al.* 2011). Furthermore, John J. Barron *et al.* (2006) proposed that the resistance of the pH sensor membrane increases when the temperature is decreased. The lower temperature of the sensing membrane, the higher membrane resistance and this would lead to a sluggish sensor response. Thus, an increase in temperature would lead to improved sensitivity. These experimental results support previous findings in the literature (Sardarinejad *et al.* 2015; Chiang *et al.* 2011; Gandía-Romero *et al.* 2016). When the temperature was below 15 °C or higher than 55 °C, the arrayed flexible IGZO pH sensor was unable to obtain a response potential in the buffer solutions from pH 1 to pH 13. As a consequence, the arrayed flexible IGZO pH sensor could only operate normally between 15 °C and 55 °C which meant that there were upper and lower temperature limits.

Average sensitivity increases slightly as temperature rises (Gandía-Romero *et al.* 2016). The average sensitivity versus temperature for the IGZO/Al pH sensor is shown in Fig. 8. The fitting curve was plotted and shows intervals of 15 °C to 35 °C, 35 °C to 55 °C and 15 °C to 55 °C. The temperature coefficients were 0.342 mV/pH °C, 0.138 mV/pH °C and 0.237 mV/pH °C. The pH sensitivity increased as the temperature of the solution increased, and from the slope of the pH sensitivity versus temperature, the temperature coefficient could be determined

(Chiang et al. 2001; Liao et al. 1998). The slope of the pH sensitivity versus temperature was obtained from the linear fit of Origin 7.0. Table 2 shows a comparison of the temperature

coefficient with different sensing membranes, and this revealed that the flexible IGZO/Al pH sensor possessed not only good sensitivity but also mass fabrication potential with a simple operation at a low cost.

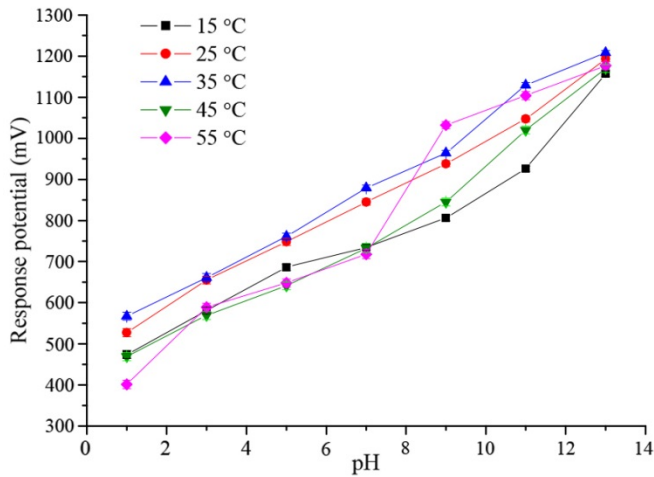


Fig. 7 The curve of response potential versus pH value for IGZO/Al pH sensor at different temperatures.

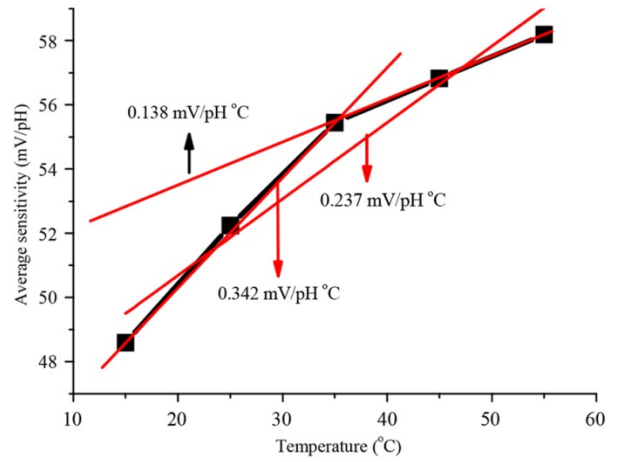


Fig. 8 The temperature coefficient of the IGZO/Al pH sensor.

Table 1 The average sensitivity and linearity of the IGZO/Al pH sensor at different temperatures.

Temperature (°C)	pH	Response potential (mean ± SD, mV)	Average sensitivity (mV/pCl)	Linearity
15	1	474 ± 9.789	48.589	0.978
	3	581 ± 8.315		
	5	686 ± 7.848		
	7	735 ± 7.217		
	9	806 ± 6.846		
	11	926 ± 6.549		
25	13	1157 ± 6.401	52.238	0.998
	1	527 ± 9.947		
	3	655 ± 9.565		
	5	748 ± 8.846		
	7	845 ± 7.217		
	9	938 ± 7.456		
35	11	1047 ± 7.649	55.446	0.993
	13	1193 ± 6.895		
	1	567 ± 9.651		
	3	661 ± 9.785		
	5	761 ± 8.235		
	7	879 ± 7.065		
45	9	964 ± 6.565	56.821	0.989
	11	1129 ± 6.355		
	13	1208 ± 5.216		
	1	469 ± 9.698		
	3	569 ± 9.569		
	5	641 ± 9.568		
55	7	733 ± 10.895	58.196	0.976
	9	845 ± 9.847		
	11	1020 ± 9.568		
	13	1170 ± 9.568		
	1	401 ± 10.232		
	3	589 ± 9.355		
5	648 ± 9.790			
7	718 ± 10.999			
9	1032 ± 9.003			
11	1104 ± 10.001			
13	1177 ± 9.786			

Table 2 The comparisons of the temperature coefficients with different sensing membranes.

Sensing membrane	Structure	pH solution	Temperature (°C)	Max sensitivity (mV/pH)	Temperature coefficient (mV/pH °C)	Linearity	Reference
IGZO/Al	Flexibility	pH1-pH13	15-55	58.196	0.237	0.976	In this study
RuO ₂	Chip	pH4-pH10	1.5-50	65.66-84.50	0.388	0.975	Sardarinejad <i>et al.</i> 2015
a-WO ₃	ISFET	pH1-pH 7	25-65	55.800	0.269	N/A	Chiang <i>et al.</i> 2001
AlN	ISFET	pH1-pH11	5-65	48.4-57.3	0.980	N/A	Chiang <i>et al.</i> 2005
AlN	ISFET	pH1-pH11	5-65	57.250	0.130	N/A	Chiang <i>et al.</i> 2012
a-Si:H	ISFET	pH2-pH9	15-65	59.970	0.240	N/A	Chou <i>et al.</i> 2001

Repeatability was measured using the potential variations in response that were determined through repeated measurement using the same device. In this study, each pH value was measured 60 times (Number of measurement), and the pH values were from pH 1 to pH 13. The experimental results of the repeatability analysis are shown in Fig. 9 and Table 3. As shown in Fig. 9, the deviation values of the pH 1, pH 3, pH 5, pH 7, pH 9, pH 11 and pH 13 buffer solutions were 2.287 mV, 1.065 mV, 2.546 mV, 2.664 mV, 8.720 mV, 3.674 mV and 5.683 mV, respectively. The SD was from 1.065 mV to 8.720 mV and this was evidence that the arrayed flexible IGZO pH sensor possessed better repeatability.

Sensitivity and linearity were not the only factors used to determine the effectiveness of the arrayed flexible IGZO pH

sensor. To determine the stability of the arrayed flexible IGZO pH sensor, drift effect, which is a non-ideal effect of the sensor, was measured (Dun *et al.* 1991). The IGZO pH sensor was immersed in a pH 7 buffer solution for 12 hr. The response voltage was stable at about 60 s, and the drift rate was calculated between 60 s and 12 hr. The experimental results in Table 4 shows that the drift rate increased as the temperature increased. The lowest drift rate was measured at 1.384 mV/hr in the pH 7 buffer solution at 15 °C, and this experimental result is shown in Fig. 10. The drifted response potential was attributed to the diffusion of ions, thereby increasing the thickness of the hydration layer on the surface of the IGZO membranes. The thickness of the hydration layer increased over time which led to voltage drift (Chou *et al.* 2000; Chou *et al.* 2014).

The hysteresis effect is another non-ideal effect of the pH sensor, and it is also referred to as the memory effect (Bousse *et al.* 1990; Lonsdale *et al.* 2017). The cycle during the hysteresis measurement was pH 7- pH 3- pH 7- pH 11- pH 7, and the hysteresis voltage was calculated as the difference between the initial and final response potentials in the pH 7 solution. The experimental results are shown in Fig. 11 and Table 5, and the hysteresis voltage was the result of a slow response of the output potential. The diffusion rate of the H⁺ ions was slow and this resulted in the slow response of the pH sensor during the change in the pH value of the buffer solution (Das *et al.* 2014). The hysteresis voltage decreased as the temperature of the pH buffer increased and this was due to the thermal convection of the solution under higher temperatures. The phenomenon of thermal convection is like flowing water, so it was able to improve the sensing characteristics of the pH sensor. The flowing pH buffer solution resulted in a decline in diffusion resistance which existed between the sensing membrane and pH buffer solution, and it also enhanced the diffusion rate of the H⁺ ions (Cheng *et al.* 2013).

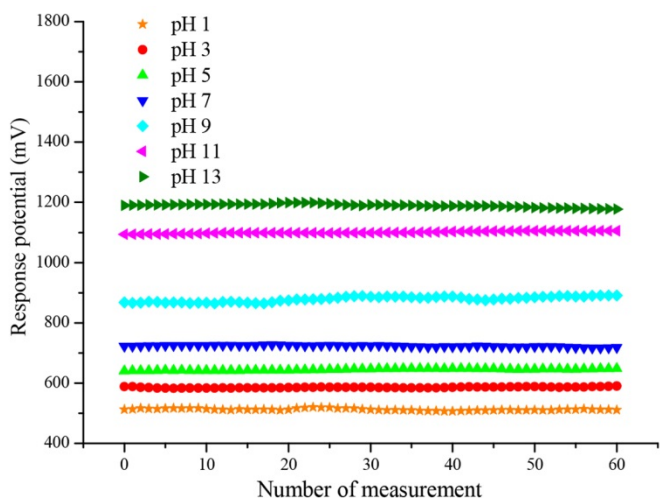


Fig. 9 The repeatability analysis of the arrayed flexible IGZO pH sensor in different pH buffer solutions at 55 °C.

Table 3 The repeatability analysis with different pH solutions at 55 °C.

pH	Average response potential (mV)	Deviation potential (mV)
1	512.095	2.287
3	585.801	1.065
5	644.911	2.546
7	723.141	2.664
9	878.860	8.720
11	1100.352	3.674
13	1189.400	5.683

Table 4 The drift rates for the different temperatures based on the arrayed flexible IGZO pH sensor.

Temperature (°C)	Drift rate (mV/hr)
15	1.384
25	3.850
35	4.857
45	6.857
55	9.857

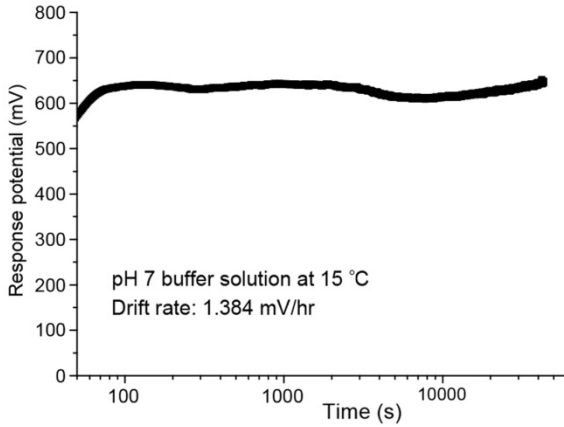


Fig. 10 The drift rate of the arrayed flexible IGZO pH sensor in pH 7 buffer solution at 15 °C.

Table 5 The hysteresis effect for the different temperatures during the cycle of pH 7- pH 3- pH 7- pH 11- pH 7.

Temperature (°C)	Hysteresis voltage (mV)
15	25.316
25	21.571
35	17.226
45	15.073
55	14.006

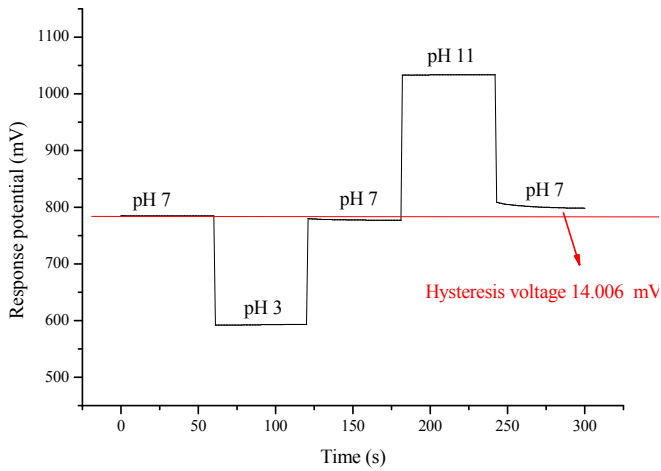


Fig. 11 The hysteresis effect of the arrayed flexible pH sensor immersed in pH buffer solution during the cycle of pH 7- pH 3- pH 7- pH 11- pH 7 at 55 °C.

4. CONCLUSION

In this study, the arrayed flexible IGZO pH sensor was fabricated, and the effect of temperature on the sensing performance of the sensor was investigated. The thickness and average roughness of the IGZO thin film were 117 nm and 8.43 nm, respectively. Temperature versus average sensitivity for the IGZO pH sensor was also investigated, and the best average sensitivity was 59.893 mV/pH at a temperature of 55 °C. The temperature coefficient from 15 °C to 55 °C was 0.237 mV/pH °C. Moreover, temperature also played a role in the drift effect and hysteresis

effect. The drift voltage increased as the temperature increased and the hysteresis voltage decreased as the temperature increased. Compared to other research in this area, the arrayed flexible IGZO pH sensor had the advantages of good stability, high sensitivity, flexibility, low cost and portability.

ACKNOWLEDGMENTS

This work was supported by Ministry of Science and Technology, Republic of China, under the Contracts MOST 106-2221-E-224-047 and MOST 107-2221-E-224-030.

REFERENCES

Amiri, M., Amali, E., Nematollahzadeh, A., and Salehniya, H. (2016). "Poly-dopamine films: voltammetric sensor for pH monitoring," *Sens. Actuators. B Chem.*, Vol. 228, pp. 53-58.

Barron, J.J., Ashton, C., and Geary, L. (2006). "The effects of temperature on pH measurement," The 57th Annual Meeting of the International Society of Electrochemistry, Edinburgh.

Bousse, L., Vlekert, H.H., and Rooij, N.F. (1990). "Hysteresis in Al₂O₃-gate ISFETs," *Sens. Actuators. B Chem.*, Vol. 2, pp. 103-110.

Cheng, T.Y., Chou, J.C., Liao, Y.H., Tsai, Y.L., Lin, J.W., Jhang, C.Y., Liu, C.Y., Hu, J.E., and Chou, H.T. (2013). "Differential reference electrode applied to arrayed pH sensor and arrayed glucose biosensor based on microfluidic framework," World Congress on Engineering, London, U.K, 5 pages, Jul. 3-5, 2013.

Chen, X.F., He, G., Liu, M., Zhang, J.W., Deng, B., Wang, P.H., Zhang, M., Lv, J.G., and Sun, Z.Q. (2014). "Modulation of optical and electrical properties of sputtering-derived amorphous InGaZnO thin films by oxygen partial pressure," *J. Alloys Compd.*, Vol. 615, pp. 636-642.

Chen, J.S., Chou, J.C., Liao, Y.H., Chen, R.T., Huang, M.S., and Wu, T.Y. (2015). "The research of the differential reference electrode arrayed flexible IGZO pH sensor for different Ar/O₂ ratios," 2015 IEEE Electron Device and Solid-State Circuits (EDSSC), Singapore, 4 pages, June 1-4, 2015.

Chen, C.C., Chen, H.I., Liu, H.Y., Chou, P.C., Liou, J.K., and Liu, W.C. (2015). "On a GaN-based ion sensitive field-effect transistor (ISFET) with a hydrogen peroxide surface treatment," *Sens. Actuators. B Chem.*, Vol. 209, pp. 658-663.

Chiang, J.L., Jan, S.S., Chou, J.C., and Chen, Y.C. (2001). "Study on the temperature effect, hysteresis and drift of pH-ISFET devices based on amorphous tungsten oxide," *Sens. Actuators. B Chem.*, Vol. 76, pp. 624-628.

Chiang, J.L., Chou, J.C., and Chen, Y.C. (2001). "Study of the pH-ISFET and EnFET for biosensor applications," *J. Med. Biol. Eng.*, Vol. 21, pp. 135-146, Jul. 2001.

Chiang, J.L., Chou, J.C., and Chen, Y.C. (2005). "Study on light and temperature properties of AlN pH-ion-sensitive field-effect transistor devices," *Jpn. J. Appl. Phys.*, Vol. 44, pp. 4831-4837.

Chiang, J.L., Chen, Y.C., Chou, J.C., and Cheng, C.C., (2012). "Temperature effect on AlN/SiO₂ gate pH-Ion-sensitive field-Effect transistor devices," *Jpn. J. Appl. Phys.*, Vol 41, pp. 541-545.

Cho, N.G. and Kim, I.D. (2011). "NO₂ gas sensing properties of amorphous InGaZnO₄ submicron-tubes prepared by polymeric fiber templating route," *Sens. Actuators. B Chem.*, Vol. 160, pp. 499-504.

Chou, J.C., Wang, Y.F., and Tsai, H.M. (2001). "Temperature dependence of surface potential in a-Si:H pH-ion sensitive field effect transistor," *Jpn. J. Appl. Phys.*, Vol. 40, pp. 3975-3978.

Chou, J.C., Huang, K.Y., and Lin, J.S. (2000). "Simulation of time-dependent effects of pH-ISFETs," *Sens. Actuators. B Chem.*, Vol.

- 62, pp. 88-91.
- Chou, J.C., Cheng, T.Y., Ye, G.C., Liao, Y.H., Yang, S.Y., and Chou, H.T. (2013). "Fabrication and investigation of arrayed glucose biosensor based on microfluidic framework," *IEEE Sens. J.*, Vol. 13, pp. 4180-4187.
- Chou, J.C., Jhang, C.Y., Liao, Y.H., Lin, J.W., Chen, R.T., and Chou, H.T. (2014). "Research of stability and interference with the potentiometric flexible arrayed glucose sensor based on microfluidic framework," *IEEE Trans. Semicond. Manuf.*, Vol. 27, pp. 523-529.
- Chou, J.C., Chen, J.S., Huang, M.S., Liao, Y.H., Lai, C.H., Wu, T.Y., and Yan, S.J. (2016). "The characteristic analysis of IGZO/Al pH sensor and glucose biosensor in static and dynamic measurements," *IEEE Sens. J.*, Vol. 16, pp. 8509-8516.
- Chou, J.C., Huang, M.S., Liao, Y.H., Lai, C.H., Chen, J.S., Chou, H.T., and Hsu, C.C. (2016). "Fabrication of the enzymatic glucose biosensor based on indium gallium zinc oxide sensing electrode," *Mater. Lett.*, Vol. 176, pp. 94-96.
- Chou, J.C., Yan, S.J., Liao, Y.H., Lai, C.H., Wu, Y.X., Wu, C.Y., Chen, H.Y., Huang, H.Y., and Wu, T.Y. (2017). "Fabrication of flexible arrayed lactate biosensor based on immobilizing LDH-NAD⁺ on NiO film modified by GO and MBs," *Sensors*, Vol. 17, pp. 12.
- Chou, J.C., Yan, S.J., Liao, Y.H., Lai, C.H., Chen, J.S., Chen, H.Y., Tseng, T.W., and Wu, T.Y. (2018). "Characterization of flexible arrayed pH sensor based on nickel oxide films," *IEEE Sens. J.*, Vol. 18, No. 2, pp. 605-612.
- Das, A., Ko, D.H., Chen, C.H., Chang, L.B., Lai, C.S., Chu, F.C., Chow, L., and Lin, R.M. (2014). "Highly sensitive palladium oxide thin film extended gate FETs as pH sensor," *Sens. Actuators. B Chem.*, Vol. 205, pp. 199-205.
- Dun, Y., Wei, Y.D., and Wang, G.H. (1991). "Time-dependent response characteristics of pH-sensitive ISFET," *Sens. Actuators. B Chem.*, Vol. 3, pp. 279-285.
- Dong, Z., Wejinya, U.C., and Elhaji, I.H. (2013). "Fabrication and testing of ISFET based pH sensors for microliter target solutions," *Sens. Actuators. A Phys.*, Vol. 194, pp. 181-187.
- Gandía-Romero, J.M., Campos, I., Valcuende, M., García-Breijo, E., Marcos, M.D., Payá, J., and Soto, J. (2016). "Potentiometric thick-film sensors for measuring the pH of concrete," *Cement Concrete Comp.*, Vol. 68, pp. 66-76.
- Khodadoust, S., Kouri, N.C., Talebayanpoor, M.S., Deris, J., and Pebdani, A.A. (2015). "Design of an optically stable pH sensor based on immobilization of Giemsa on triacetylcellulose membrane," *Mater. Sci. Eng. C*, Vol. 57, pp. 304-308.
- Liao, H.K., Chou, J.C., Chung, W.Y., Sun, T.P., and Hsiung, S.K. (1998). "Study of amorphous tin oxide thin films for ISFET applications," *Sens. Actuators. B Chem.*, Vol. 50, pp. 104-109.
- Lonsdale, W., Maurya, D.K., Wajrak, M., Tay, C.Y., Marshall, B.J., and Alameh, K. (2017). "Rapid measurement of urease activity using a potentiometric RuO₂ pH sensor for detection of *Helicobacter pylori*," *Sens. Actuators. B Chem.*, Vol. 242, pp. 1305-1308.
- Manjakkal, L., Djurdjic, E., Cvejic, K., Kulawik, J., Zaraska, K., and Szwagierczak, D. (2015). "Electrochemical impedance spectroscopic analysis of RuO₂ based thick film pH sensors," *Electrochim. Acta*, Vol. 168, pp. 246-255.
- Manjakkal, L., Zaraska, K., Cvejic, K., Kulawik, J., and Szwagierczak, D. (2016). "Potentiometric RuO₂-Ta₂O₅ pH sensors fabricated using thick film and LTCC technologies," *Talanta*, Vol. 147, pp. 233-240.
- Nor, N.M., Lockman, Z., and Razak, K.A. (2015). "Study of ITO glass electrode modified with iron oxide nanoparticles and nafion for glucose biosensor application," *Procedia Chem.*, Vol. 19, pp. 50-56.
- Rahimi, R., Ochoa, M., Parupudi, T., Zhao, X., Yazdi, I.K., Dokmeci, M.R., Tamayol, A., Khademhosseini, A., and Ziaie, B. (2016). "A low-cost flexible pH sensor array for wound assessment," *Sens. Actuators. B Chem.*, Vol. 229, pp. 607-617.
- Singh, S. (2016). "Al doped ZnO based metal-semiconductor-metal and metal-insulator-semiconductor-insulator-metal UV sensors," *Optik*, Vol. 127, pp. 3523-3526.
- Sardarinejad, A., Maurya, D.K., Khaled, M., and Alameh, K. (2015). "Temperature effects on the performance of RuO₂ thin-film pH sensor," *Sens. Actuators. A Phys.*, Vol. 233, pp. 414-421.
- Tyagi, P., Sharma, A., Tomar, M., and Gupta, V. (2016). "Metal oxide catalyst assisted SnO₂ thin film based SnO₂ gas sensor," *Sens. Actuators. B Chem.*, Vol. 224, pp. 282-289.
- Uria, N., Abramova, N., Bratov, A., Pascual, F.X.M., and Baldrich, E. (2016). "Miniaturized metal oxide pH sensors for bacteria detection," *Talanta*, Vol. 147, pp. 364-369.
- Yang, D.J., Whitfield, G.C., Cho, N.G., Cho, P.S., Kim, I.D., Saltsburg, H.M., and Tuller, H.L. (2012). "Amorphous InGaZnO₄ films: Gas sensor response and stability," *Sens. Actuators. B Chem.*, Vol. 171-172, pp. 1166-1171.
- Yang, C.M., Wang, J.C., Chiang, T.W., Lin, Y.T., Juan, T.W., Chen, T.C., Shih, M.Y., Lue, C.E. and Lai, C.S. (2013). "Nano-IGZO layer for EGFET in pH sensing characteristics," 2013 IEEE 5th International Nanoelectronics Conference (INEC), pp. 480-482, Singapore, 2-4 Jan. 2013.
- Yaqoob, U., Phan, D.T., Uddin, A.S.M.I., and Chung, G.S. (2015). "Highly flexible room temperature NO₂ sensor based on MWCNTs-WO₃ nanoparticles hybrid on a PET substrate," *Sens. Actuators. B Chem.*, Vol. 221, pp. 760-768.
- Zubiatega, P., Zamarreño, C.R., Del Villar, I., Matias, I.R., and Arregui, F.J. (2016). "Tunable optical fiber pH sensors based on TE and TM Lossy Mode Resonances (LMRs)," *Sens. Actuators. B Chem.*, Vol. 231, pp. 484-490.